

### Beta-Decay Matrix Elements in $Sb^{122}\dagger^*$

G. E. BRADLEY,<sup>†</sup> F. M. PIPKIN,<sup>§</sup> AND R. E. SIMPSON<sup>||</sup>  
 Lyman Laboratory, Harvard University, Cambridge, Massachusetts  
 (Received February 6, 1961)

Dynamic nuclear orientation has been used to study the  $2^- \leftrightarrow 2^+$  1.42-Mev beta ray in the decay of  $Sb^{122}$ . The  $Sb^{122}$ , which was a substitutional donor atom in a silicon crystal, was oriented by saturating each of the four  $\Delta(m_I + m_J) = 0$  forbidden transitions. The angular distribution of the gamma ray following the beta ray was measured with two scintillation counters. The nuclear and electron relaxation times were determined by the rate of growth and decay of the nuclear orientation. The electron ( $\Delta m_J = \pm 1, \Delta m_I = 0$ ) relaxation time was found to be  $(4.9 \pm 1.2)$  min. The nuclear relaxation can be represented as due to a combination of the modulation of the isotropic hyperfine interaction and nuclear quadrupole relaxation. For the dipole mechanism,  $50 \text{ min} \leq T_N \leq 100 \text{ min}$  and for the quadrupole mechanism,

$150 \text{ min} \leq T_N \leq 1700 \text{ min}$ . An analog computer was used to correct the initial orientation parameters for the effects of nuclear relaxation. From these, data restrictions can be placed upon the relative amounts of angular momentum carried off by the 1.42-Mev  $\beta$  ray. The modified  $B_{ij}$  approximation was then used to analyze this result in conjunction with the beta-gamma angular correlation. There are three sets of matrix elements which can explain the observed data. One set implies that all the antimony atoms are in the simple donor sites; the other two sets imply that only 40% of the antimony atoms are in the donor sites. The first set gives  $V = -0.5 \pm 0.1, Y = -0.5 \pm 0.1$ ; the second set,  $V = -4.2 \pm 2.0, Y = -1.4 \pm 0.5$ ; the third set,  $V = -6.3 \pm 1.0, Y = +1.8 \pm 1.5$ .

**T**HIS paper reports the use of dynamic nuclear orientation to study the  $2^- \leftrightarrow 2^+$  first-forbidden beta transition in  $Sb^{122}$ . There are, in general, six nuclear matrix elements which can contribute to this decay; two which carry off no angular momentum, three which carry off one unit of angular momentum, and one which carries off two units of angular momentum. In this experiment the  $Sb^{122}$  nuclei in the ground state are oriented and the angular distribution of the gamma ray following the first-forbidden beta ray is observed. The orientation parameters of the initial state can be calculated from the known method of orientation and the measured nuclear relaxation times; the orientation parameters of the daughter state are determined from the gamma-ray angular distribution. The change of orientation parameters due to the beta decay can consequently be determined. This change depends upon the angular momentum carried off by the electron-neutrino system. The method of analysis of the data is similar to that used for  $As^{76}$ . Since this has been described elsewhere,<sup>1</sup> only an outline of the theory will be included here.

#### REVIEW OF THE THEORY

##### A. Description of Nuclear Orientation

The decay scheme of 65-hr  $Sb^{122}$  has been extensively investigated by many workers, among whom the principal ones are Glaubman<sup>2</sup> and Farrelly *et al.*<sup>3</sup> The

<sup>†</sup> This research was supported by a grant from the National Science Foundation.

<sup>\*</sup> This paper is in part based on a thesis submitted by one of the authors (R.E.S.) to Harvard University in partial fulfillment of the requirements for the degree of Doctor of Philosophy.

<sup>†</sup> Research performed while a National Science Foundation Faculty Fellow on leave from Western Michigan University.

<sup>§</sup> Alfred P. Sloan Research Fellow, 1959-61.

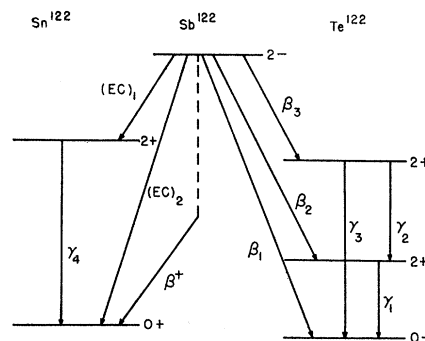
<sup>||</sup> Now at University of Alaska, College Park, Alaska.

<sup>1</sup> F. M. Pipkin, G. E. Bradley, and R. E. Simpson, *Nuclear Phys.* (to be published).

<sup>2</sup> M. J. Glaubman, *Phys. Rev.* **98**, 645 (1955).

<sup>3</sup> B. Farrelly, L. Koerts, N. Benczer, R. van Lieshout, and C. S. Wu, *Phys.* **99**, 1440 (1955).

decay scheme which is given by the most recent set of Nuclear Data Cards<sup>4</sup> is shown in Fig. 1. The unique first-forbidden shape of the 1.97-Mev beta ray leads to the assignment of spin 2 and negative parity to the ground state of  $Sb^{122}$ . This is confirmed by the comparison of the experimental and theoretical  $K$  capture ratios for the  $Sb^{122}$ - $Sn^{122}$  ground-state transition,<sup>5</sup> and by a previous orientation experiment.<sup>6</sup> The spin and parity assignments for the excited states of  $Te^{122}$  have been made from a study of the beta-gamma and



RADIATION	ENERGY	INTENSITY	LOG f1
$\beta_1$	1.97	30.0 %	8.4
$\beta_2$	1.40	62.9 %	7.6
$\beta_3$	0.74	4.0 %	7.7
$\beta^+$	~0.57	0.0063 %	—
$(EC)_1$	0.7	0.8 %	—
$(EC)_2$	1.45	2.3 %	—
$\gamma_1$	0.564	66.4 %	EQ
$\gamma_2$	0.686	3.4 %	EQ+MD
$\gamma_3$	1.26	0.7 %	EQ
$\gamma_4$	1.14	0.73 %	EQ

FIG. 1. Nuclear energy level diagram for  $Sb^{122}$ .

<sup>4</sup> Nuclear Data Cards prepared by National Research Council, pp. 58-4-7.

<sup>5</sup> M. L. Perlman, J. P. Welker, and M. Wolfsberg, *Phys. Rev.* **110**, 381 (1958).

<sup>6</sup> F. M. Pipkin, *Phys. Rev.* **112**, 935 (1958).

gamma-gamma angular correlations.<sup>7-9</sup> The radiations  $\gamma_1$  and  $\gamma_3$  are pure electric quadrupole; the radiation  $\gamma_2$  is a mixture of (92±4)% electric quadrupole and (8±4)% magnetic dipole. The mean life of the 564-kev state of Te<sup>122</sup> has been found to be 2.2×10<sup>-10</sup> sec by a coincidence technique<sup>10</sup> and 1.4×10<sup>-11</sup> sec by a study of the Coulomb excitation of the 564-kev level.<sup>11</sup>

The 1.40-Mev beta ray ( $\beta_2$ ) is a first-forbidden transition with an allowed spectrum shape. The  $\beta_2$ - $\gamma_1$  angular correlation has been measured<sup>12</sup> for beta rays of energy 1 to 1.4 Mev the angular correlation is

$$1 + (0.099 \pm 0.013)P_2(\cos\theta). \quad (1)$$

Somoilov *et al.*<sup>13</sup> have oriented Sb<sup>122</sup> by an adiabatic demagnetization experiment. In their experiment the antimony was an impurity atom in an iron lattice. In this environment there exists a magnetic field of the order of 200 to 300 kgauss at the antimony nucleus. The antimony atoms were cooled by placing the iron foil in thermal contact with a paramagnetic salt which could be cooled by demagnetization. The result of their experiment can be expressed in terms of the observed gamma-ray angular distribution,

$$W(\theta) = 1 - \frac{(2.2 \pm 0.2) \times 10^{-5}}{T^2} P_2(\cos\theta), \quad (2)$$

where  $T$  is the absolute temperature.

In the experiment reported in this paper, the angular distribution of the gamma rays from dynamically oriented Sb<sup>122</sup> is observed. It is desired to deduce the orientation parameters of nuclei which have reached the 564-kev level via the emission of  $\beta_2$ . The angular distribution of those  $\gamma_1$  which follow  $\beta_2$  is<sup>14</sup>

$$W(\theta) = 1 - (10/7)B_2 f_2 P_2(\cos\theta) - (40/3)B_4 f_4 P_4(\cos\theta), \quad (3)$$

where

$$f_2 = \frac{1}{j_0^2} \sum_{m_0} m_0^2 (a_{m_0} - \frac{1}{5}),$$

$$f_4 = \frac{1}{j_0^4} \sum_{m_0} m_0^2 \left( m_0^2 - \frac{31}{7} \right) (a_{m_0} - \frac{1}{5}),$$

and

$$P_2(\cos\theta) = \frac{3}{2}(\cos^2\theta - \frac{1}{3}),$$

$$P_4(\cos\theta) = (35/8)[\cos^4\theta - (6/7)\cos^2\theta + (3/35)].$$

<sup>7</sup> F. Lindquist and J. Marklund Nuclear Phys. 4, 189 (1957).  
<sup>8</sup> C. F. Coleman, Nuclear Phys. 5, 495 (1958).  
<sup>9</sup> I. Asplund, L. G. Strömberg, and T. Wiedling, Arkiv Fysik 18, 65 (1960).

<sup>10</sup> C. F. Coleman, Phil. Mag. 46, 1135 (1955).  
<sup>11</sup> G. M. Temmer and N. P. Heydenburg, Phys. Rev. 104, 967 (1956).

<sup>12</sup> I. Shakhov, Phys. Rev. 82, 333(A) (1951).  
<sup>13</sup> B. N. Somoilov, V. V. Sklyarevskii, and E. P. Stepanov, Soviet Phys.-JETP 11, 261 (1960).

<sup>14</sup> S. R. de Groot and H. A. Tolhoek in *Beta- and Gamma-Ray Spectroscopy*, edited by K. Siegbahn (North-Holland Publishing Company, Amsterdam, 1955), Chap. 19, Part III, p. 613.

The parameters  $B_2$  and  $B_4$  are attenuation factors which depend upon the angular momentum carried off by the electron-neutrino system. If  $\alpha_0$ ,  $\alpha_1$ , and  $\alpha_2$  represent the relative probabilities that the beta ray carries off angular momenta, 0, 1, and 2, respectively, then

$$B_2 = 1 - (\alpha_1/2) - (17\alpha_2/14), \quad (4)$$

$$B_4 = 1 - (5\alpha_1/3) - (5\alpha_2/7), \quad (5)$$

where  $\alpha_0 + \alpha_1 + \alpha_2 = 1$ . The principal object of this experiment is to determine  $B_2$  and  $B_4$  and from them  $\alpha_0$ ,  $\alpha_1$ , and  $\alpha_2$ . In describing the orientation it is sometimes advantageous to speak of the signals  $S(\theta) = W(\theta) - 1$  and the nuclear polarization

$$f_1 = \frac{1}{j_0} \sum_{m_0} m_0 (a_{m_0} - \frac{1}{5}).$$

The angular distribution of  $\gamma_3$  will be given by an identical expression with  $B_2$  and  $B_4$  replaced by  $B_2'$  and  $B_4'$ , the parameters which characterize  $\beta_3$ . In a similar fashion  $\gamma_4$  can be characterized by  $B_2''$  and  $B_4''$ . The angular distribution of  $\gamma_2$  will be<sup>15</sup>

$$W(\theta) = 1 + \frac{1}{21} \left[ -21a_1^2 + 126 \left( \frac{5}{21} \right)^{\frac{1}{2}} a_1 a_2 + \frac{45}{7} a_2^2 \right] \times f_2 B_2' P_2(\cos\theta) - \frac{80}{21} a_2^2 f_4 B_4' P_4(\cos\theta), \quad (6)$$

where  $a_1$  and  $a_2$  are the reduced matrix elements for the magnetic dipole and electric quadrupole components of  $\gamma_2$  normalized so that

$$a_1^2 + a_2^2 = 1.$$

For Sb<sup>122</sup>,<sup>7-9</sup>

$$a_2/a_1 = \delta = +3.5 \pm 0.4.$$

The angular distribution for those  $\gamma_1$  which follow  $\gamma_2$  is

$$W(\theta) = 1 - (10/7)[(a_1^2/2) - (3a_2^2/14)]f_2 B_2' P_2(\cos\theta) - (40/3)[-(2a_1^2/3) + (2a_2^2/7)]f_4 B_4' P_4(\cos\theta). \quad (7)$$

If it is assumed that all the  $\gamma$  rays are counted with the same efficiency, then the intensity of the gamma rays given in Fig. 1 can be used to compute the total angular distribution. The result of this calculation is

$$W(\theta) = 1 - (10/7)[0.897B_2 - 0.030B_2' + 0.010B_2''] \times f_2 P_2(\cos\theta) - (40/3)[0.897B_2 - 0.032B_4' + 0.010B_4'']f_4 P_4(\cos\theta). \quad (8)$$

### B. Initial Orientation Parameters

In order to find the initial orientation parameters, we must consider the mechanism of orientation and the

<sup>15</sup> C. D. Hartogh, H. A. Tolhoek, and S. R. de Groot, Physica 20, 1310 (1954).

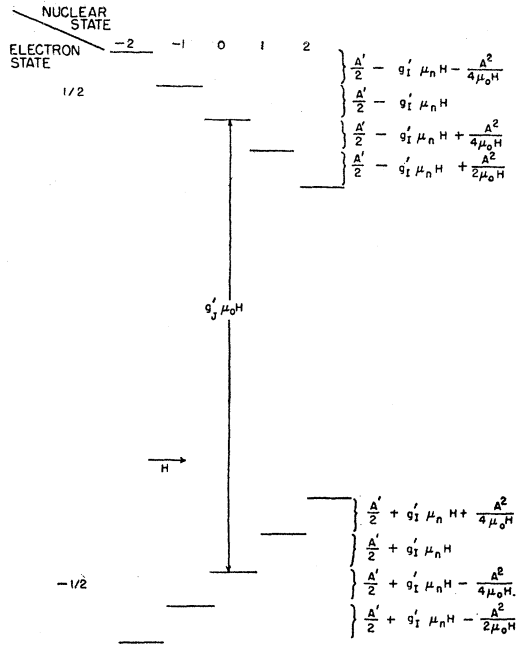


FIG. 2. Energy levels of the Sb<sup>122</sup> donor atom in a silicon crystal. The arrow with an *H* indicates the order in which the transitions occur with fixed oscillator frequency and increasing magnetic field.

manner in which the nuclear relaxation can change the orientation parameters. The energy levels of the antimony donor atom are shown in Fig. 2. The orientation is produced by the saturation of the  $\Delta(m_I+m_J)=0$  forbidden transitions. This process of production of the orientation is shown schematically in Fig. 3. If the only relaxation were due to electron spin translations ( $\Delta m_J = \pm 1, \Delta m_I = 0$ ), then saturation of the four forbidden transitions would result in the equilibrium values of  $f_2$  and  $f_4$  shown in Table I. Nuclear relaxation will cause the  $f_2$  and  $f_4$  to depart from these values.

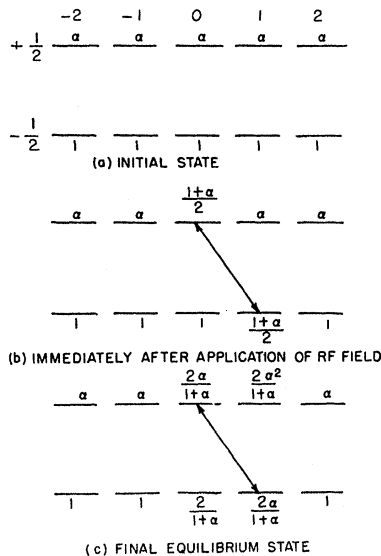


FIG. 3. Schematic representation of the formation of the nuclear orientation by saturation of a forbidden transition. The symbol  $\alpha$  stands for  $e^{-(2\mu_0 H/kT)}$ .

If the relative populations of the various magnetic substates are  $P(m_J, m_I)$ , where

$$\sum_{m_I, m_J} P(m_J, m_I) = 1,$$

then the change in time of these populations can be described by the set of equations<sup>6</sup>

$$\begin{aligned} \dot{P}_{m_J, m_I} = & \sum_{m_I', m_J'} W(m_J, m_I | m_J', m_I') \\ & \times \{ \exp[-(\mu_0 H/kT)(m_J - m_J')] P(m_J', m_I') \\ & - \exp[-(\mu_0 H/kT)(m_J' - m_J)] P(m_J, m_I) \}. \end{aligned} \quad (9)$$

In this expression  $W(m_J, m_I | m_J', m_I')$  are coefficients which determine the relaxation rate. For an atomic spin of  $\frac{1}{2}$  they can be expressed in terms of the Clebsch-Gordan coefficients. For the analysis of the antimony

TABLE I. The  $f_2$  and  $f_4$  parameters for saturation of the four  $\Delta(m_I+m_J)=0$  forbidden transitions. It has been assumed that there is no nuclear relaxation and that the time of application of the radiofrequency field is much longer than the electron relaxation time.

Transition	$f_2$	$f_4$
$(-\frac{1}{2}, -1) \rightarrow (\frac{1}{2}, -2)$	$\frac{3}{20} \tanh \frac{\mu_0 H}{kT}$	$\frac{3}{140} \tanh \frac{\mu_0 H}{kT}$
$(-\frac{1}{2}, 0) \rightarrow (\frac{1}{2}, -1)$	$\frac{1}{20} \tanh \frac{\mu_0 H}{kT}$	$-\frac{3}{70} \tanh \frac{\mu_0 H}{kT}$
$(-\frac{1}{2}, 1) \rightarrow (\frac{1}{2}, 0)$	$-\frac{1}{20} \tanh \frac{\mu_0 H}{kT}$	$\frac{3}{70} \tanh \frac{\mu_0 H}{kT}$
$(-\frac{1}{2}, 2) \rightarrow (\frac{1}{2}, 1)$	$-\frac{3}{20} \tanh \frac{\mu_0 H}{kT}$	$-\frac{3}{140} \tanh \frac{\mu_0 H}{kT}$

it will be assumed that the following relaxation mechanisms are present:

- (a) Pure electron relaxation ( $\Delta m_I = 0, \Delta m_J = \pm 1$ ).

$$W(m_J, m_I | m_J', m_I') = W_1 \delta_{m_I, m_I'} (1 - \delta_{m_J, m_J'}). \quad (10)$$

- (b) Nuclear relaxation through modulation of the isotropic hyperfine interaction.

$$\begin{aligned} W(m_J, m_I | m_J', m_I') &= W_2 (I 1 m_I' \mu | I 1 m_I)^2 \\ &\times (1 - \delta_{m_J, m_J'}) \delta_{m_I + m_J, m_I' + m_J'}. \end{aligned} \quad (11)$$

- (c) Nuclear quadrupole relaxation.

$$\begin{aligned} W(m_J, m_I | m_J', m_I') &= W_3 (I 2 m_I' \mu | I 2 m_I)^2 \delta_{m_J, m_J'} (1 - \delta_{m_I, m_I'}). \end{aligned} \quad (12)$$

For a general mixture of relaxation mechanisms, the behavior of the nuclear populations as a function of time will be rather complicated and some form of

computer is useful in solving the equations. There are two simple cases, however, which can easily be solved and which serve as a guide in determining the relaxation times. In both of these cases it is assumed the the electron relaxation time is much shorter than the nuclear relaxation time. For the formation of the orientation.

$$\begin{aligned} f_2(t) &= f_2(\infty)(1 - \frac{1}{2}e^{-\lambda_R t}), \\ f_4(t) &= f_4(\infty)(1 - \frac{1}{2}e^{-\lambda_R t}), \end{aligned} \tag{13}$$

when  $\lambda_R = 1/2T_S$  and  $T_S$  is the electron relaxation time as it is customarily defined.<sup>16</sup> For the decay of the orientation,

$$\begin{aligned} f_1(t) &= f_1(0)e^{-\lambda_1 t}, \\ f_2(t) &= f_2(0)e^{-\lambda_2 t}, \\ f_4(t) &= f_4(0)e^{-\lambda_4 t}, \end{aligned} \tag{14}$$

where  $\lambda_1, \lambda_2,$  and  $\lambda_4$  depend upon the relaxation mechanism. For a dipole relaxation mechanism, of which the hyperfine relaxation is an example,

$$\begin{aligned} \lambda_1 &= \frac{1}{12}W_2 \operatorname{sech}(\mu_0 H/kT), \\ \lambda_2 &= \frac{1}{4}W_2 \operatorname{sech}(\mu_0 H/kT), \\ \lambda_4 &= \frac{5}{8}W_2 \operatorname{sech}(\mu_0 H/kT), \end{aligned} \tag{15}$$

For the quadrupole mechanism,<sup>17</sup>

$$\begin{aligned} \lambda_1 &= W_3/2, \\ \lambda_2 &= (17/14)W_3, \\ \lambda_4 &= (5/7)W_3. \end{aligned} \tag{16}$$

Thus by observing the decay of the orientation, the relaxation time can be measured and the relaxation mechanism discovered.

To solve the more general problem it is convenient to use an analog computer. The equations for the relaxation can be duplicated by a system of condensers and resistors. The circuit for the electron relaxation plus the modulation of the isotropic hyperfine interaction is shown in Fig. 4; that for the electron relaxation plus the quadrupole relaxation in Fig. 5. In this analog the charge on the condensers corresponds to the populations of the levels. In terms of the resistors and capacitors,

$$\begin{aligned} \lambda_1 &= -\frac{1}{3} \left( \frac{1}{1+\alpha} \right) \frac{1}{R_2 C}, \\ \lambda_2 &= -\frac{1}{2} \left( \frac{1}{1+\alpha} \right) \frac{1}{R_2 C}, \\ \lambda_4 &= -\frac{5}{3} \left( \frac{1}{1+\alpha} \right) \frac{1}{R_2 C}, \end{aligned} \tag{17}$$

<sup>16</sup> J. W. Culvahouse and F. M. Pipkin, Phys. Rev. **109**, 319 (1958).

<sup>17</sup> The expressions quoted for  $\lambda_2$  and  $\lambda_4$  in references 6 and 16 are interchanged.

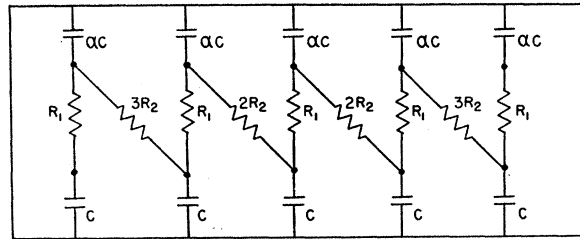


FIG. 4. Analog circuit for nuclear relaxation due to modulation of isotropic hyperfine interaction plus electron spin relaxation. The symbol  $\alpha$  is an abbreviation for  $e^{-(2\mu_0 H/kT)}$ .

for Fig. 4, and

$$\begin{aligned} \lambda_1 &= -\frac{7}{6} \frac{1}{R_3 C}, \\ \lambda_2 &= -\frac{17}{6} \frac{1}{R_3 C}, \\ \lambda_4 &= -\frac{5}{3} \frac{1}{R_3 C}, \end{aligned} \tag{18}$$

for Fig. 5. The detailed circuit which was used to analyze the experiment is described elsewhere.<sup>1</sup>

EXPERIMENTAL PROCEDURE

After neutron activation in the materials testing reactor at Arco, Idaho, the sample was annealed for five hours at 1100–1200°C to heal the radiation damage. It was placed in the rectangular microwave cavity and the wave guide assembly was inserted into the helium filled Dewar. Two integral discriminators were used with each NaI(Tl) scintillation detector, one set below the 564-keV gamma-ray photopeak and the other set just above this photopeak. A vacuum was pumped on the helium to reduce the temperature to 1.15°C. A well-coupled cavity mode was located and the

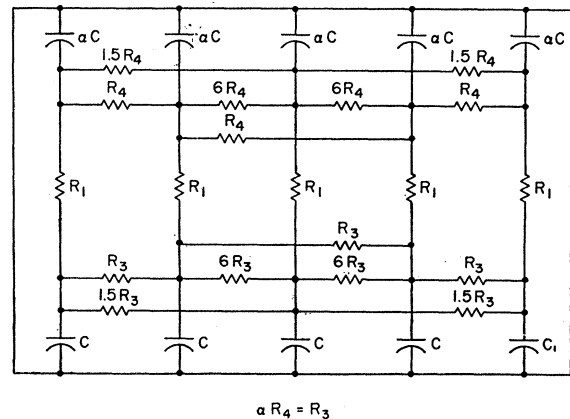


FIG. 5. Analog circuit for nuclear relaxation due to nuclear quadrupole interaction plus electron spin relaxation. The symbol  $\alpha$  is an abbreviation for  $e^{-(2\mu_0 H/kT)}$ .

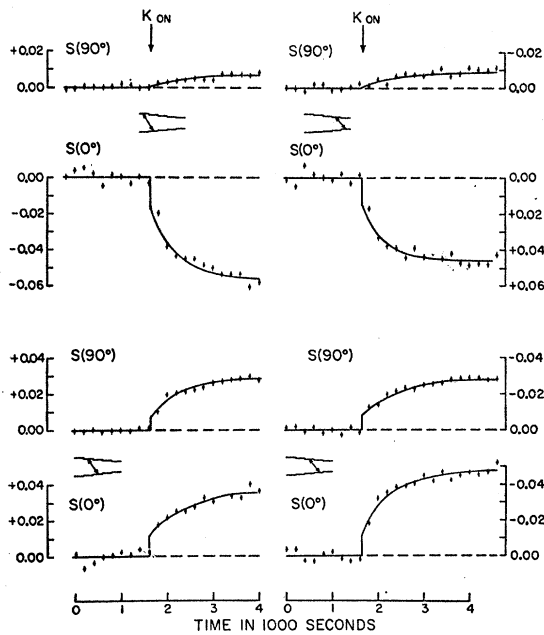


FIG. 6. A plot of the counting rates versus time for both  $90^\circ$  and  $0^\circ$  positions and for each forbidden transition. The curves are just drawn through the points and do not represent a theoretical prediction. The silicon sample (S-2) had a concentration of approximately  $3 \times 10^{16}$  donors/cm<sup>3</sup> and was irradiated for a 48-hr period in a flux of  $10^{14}$  thermal neutrons/sec cm<sup>2</sup>. It had never been irradiated before.

positions of the four forbidden lines were calculated. At this point the klystron was turned off and the magnetic field at the sample was reduced to zero for a five minute period to establish initially an isotropic nuclear population. The magnetic field was turned

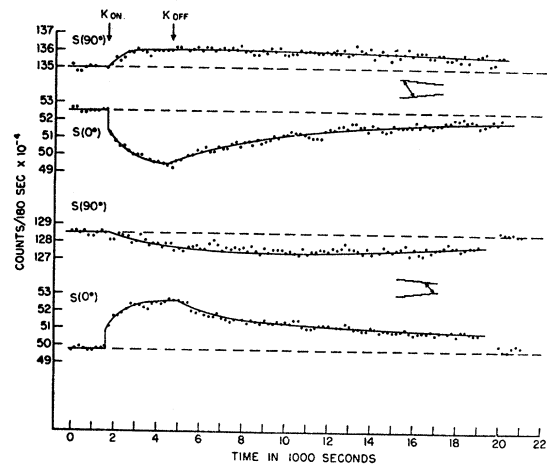


FIG. 7. The long runs which were used to determine the relaxation times for S-2. The change in counting rate at the end shows where the magnet was turned off to relax the sample.

on and adjusted so that one of the forbidden transitions was in resonance. The counting rates were then recorded for a period sufficient to establish a good reference level and the klystron was turned on. The klystron was left on until the counting rates no longer appeared to be changing. At this point the klystron was turned off and the decay of the orientation observed.

Three sources were used in this experiment. The first (S-1) was doped with  $6 \times 10^{16}$  antimony atoms/cm<sup>3</sup> and it was irradiated for a period of 44 hr in a flux of  $10^{14}$  thermal neutrons/cm<sup>2</sup> sec. The second (S-2) was doped with  $3 \times 10^{16}$  Sb/cm<sup>3</sup> and it was irradiated for 48 hr in a flux of  $10^{14}$  thermal neutrons/cm<sup>2</sup> sec. The third (S-3) was the old (S-1) source and it was ir-

TABLE II. Data on the S-3 Sb source. This crystal had a concentration of  $6 \times 10^{16}$  donors/cm<sup>2</sup> and was irradiated for a period of 96 hr in a flux of  $10^{14}$  thermal neutrons/cm<sup>2</sup> sec. The initial signals refer to the change in the orientation immediately after the radio-frequency field is turned on and before the slow rise. According to the simple theory which neglects nuclear relaxation these initial signals should be equal to one-half the final signals.

Transition	Run	H in gauss	Temp. in °K	Initial signals in %		Final signals in %	
				S(90°)	S(0°)	S(90°)	S(0°)
$(-\frac{1}{2}, 2) \rightarrow (\frac{1}{2}, 1)$	5-28	8006	1.12	0.0 ± 0.2	2.41 ± 0.20	-0.77 ± 0.2	4.78 ± 0.24
	5-62	8483	1.12	0.0 ± 0.2	1.94 ± 0.10	-0.21 ± 0.2	4.65 ± 0.13
	5-74	7898	1.12	-0.11 ± 0.11	2.91 ± 0.20	-0.43 ± 0.2	4.82 ± 0.25
$(-\frac{1}{2}, -1) \rightarrow (\frac{1}{2}, -2)$	5-54	8367	1.15	0.0 ± 0.2	-2.89 ± 0.20	+0.97 ± 0.18	-5.56 ± 0.30
	5-20	7866	1.12	0.0 ± 0.2	-3.16 ± 0.20	+0.63 ± 0.10	-6.18 ± 0.37
	5-70	7759	1.15	0.0 ± 0.15	-2.13 ± 0.16	+0.91 ± 0.15	-5.24 ± 0.16
$(-\frac{1}{2}, 1) \rightarrow (\frac{1}{2}, 0)$	5-48	8464	1.15	-1.48 ± 0.17	-2.95 ± 0.17	-2.46 ± 0.18	-4.68 ± 0.18
	5-60	8464	1.12	-1.36 ± 0.12	-3.07 ± 0.12	-2.64 ± 0.12	-4.92 ± 0.12
	5-58	8464	1.12	-1.52 ± 0.20	-3.07 ± 0.12	-2.64 ± 0.24	-5.17 ± 0.12
	5-24	7959	1.12	-1.24 ± 0.24	-2.68 ± 0.12	-1.96 ± 0.24	-4.50 ± 0.12
$(-\frac{1}{2}, 0) \rightarrow (\frac{1}{2}, -1)$	5-44	8415	1.15	1.81 ± 0.11	2.04 ± 0.15	3.69 ± 0.11	2.89 ± 0.23
	5-34	7912	1.15	0.77 ± 0.10	0 ± 0.10	2.92 ± 0.10	1.96 ± 0.10
	5-78	7806	1.15	2.25 ± 0.10	1.68 ± 0.10	3.23 ± 0.10	2.84 ± 0.10
$(\frac{1}{2}, 0) \rightarrow (-\frac{1}{2}, 0)$	5-64	8436	1.12	0.28 ± 0.12	0.0 ± 0.20	1.118 ± 0.12	0.0 ± 0.20
	5-76	7830	1.15	0.0 ± 0.15	0.0 ± 0.20	1.138 ± 0.15	0.713 ± 0.20
$(\frac{1}{2}, -1) \rightarrow (-\frac{1}{2}, -1)$	5-80	7781	1.15	0.0 ± 0.20	0.0 ± 0.20	0.099 ± 0.20	1.392 ± 0.20

radiated again for 96 hr in a flux of 10<sup>14</sup> thermal neutrons/cm<sup>2</sup> sec. A period of two months elapsed between the two irradiations.

ANALYSIS OF THE DATA

In order to determine the true angular distribution, the counting rates must be corrected for counts due to Sb<sup>124</sup>, for the counting rate loss, and for the finite solid angle subtended by the counters. The fraction of the counts due to Sb<sup>124</sup> was determined by observing the counting rate in the two channels over a period of ten days to two weeks. The counting rates versus time were then plotted on semilog paper and the fraction of the source which was Sb<sup>124</sup> was determined. Independent measurements on Sb<sup>124</sup> alone showed that there were no observable (>0.5%) radio-frequency-produced anisotropies which would confuse the measurements. The data were also corrected for the decay of the Sb<sup>122</sup>. Figure 6 shows one run for each of the forbidden transitions for source S-2. Figure 7 shows two of the long runs used to measure the nuclear relaxation times for source S-2. Data taken on source S-3 are shown in Table II. These data illustrate the reproducibility of the measurements.

A numerical integration was used to correct for the finite solid angle of the counters. These correction factors can be expressed as attenuation coefficients S<sub>2</sub>, S<sub>4</sub> in the angular distribution

$$W(\theta) = 1 - (10/7)S_2B_2f_2P_2(\cos\theta) - (40/3)S_4B_4f_4P_2(\cos\theta). \quad (19)$$

The values of S<sub>2</sub> and S<sub>4</sub> for the various sources are shown in Table III.

The electron relaxation time was determined by fitting the rise of the signals to an expression of the form

$$A - Be^{-\lambda t}.$$

The data were then analyzed into B<sub>2</sub>f<sub>2</sub> and B<sub>4</sub>f<sub>4</sub> components and the nuclear relaxation was investigated

TABLE III. Solid-angle correction factors.

Source	0° counter		90° counter	
	S <sub>2</sub>	S <sub>4</sub>	S <sub>2</sub>	S <sub>4</sub>
S-1	0.884	0.655	0.921	0.831
S-2	0.924	0.763	0.871	0.621
S-3	0.924	0.763	0.935	0.795

by fitting the decay of the B<sub>2</sub>f<sub>2</sub> and B<sub>4</sub>f<sub>4</sub> to curves of the form

$$B_2f_2 = (B_2f_2)_0 e^{-\lambda_2 t},$$

$$B_4f_4 = (B_4f_4)_0 e^{-\lambda_4 t}.$$

The average results of these calculations for each of the transitions and for each source is shown in Table IV.

The average rise constant for all three sources is

$$\lambda_R = (1.7 \pm 0.4) \times 10^{-3} \text{ sec}^{-1}.$$

This implies that the electron relaxation time is

$$T_S = (4.9 \pm 1.2) \text{ min.}$$

From the λ<sub>2</sub> and λ<sub>4</sub> derived for each transition, W<sub>2</sub> and W<sub>4</sub> can be determined. The average value for W<sub>2</sub> obtained in this fashion is

$$W_2 = (3.2 \pm 1.0) \times 10^{-4} / \text{sec.}$$

The average value of W<sub>3</sub> is

$$W_3 = (1.2 \pm 1.0) \times 10^{-4} / \text{sec.}$$

The corresponding relaxation times for the nuclear polarization can be found from Eqs. (15) and (16). For the modulation of the isotropic hyperfine interaction the nuclear relaxation time is

$$50 \text{ min} \leq T_N \leq 100 \text{ min,}$$

and for the quadrupole relaxation

$$150 \text{ min} \leq T_N \leq 1700 \text{ min.}$$

TABLE IV. The average values of B<sub>2</sub>f<sub>2</sub> and B<sub>4</sub>f<sub>4</sub>, the rise constant λ<sub>R</sub>, and the decay constants λ<sub>2</sub> and λ<sub>4</sub> obtained from all three sources. The errors are based upon the spread of the various measurements. The total spread of the B<sub>2</sub>f<sub>2</sub> and B<sub>4</sub>f<sub>4</sub> values for one source was about 10%; this is taken as an estimate of their error.

Transition	Source	B <sub>2</sub> f <sub>2</sub> in %	B <sub>4</sub> f <sub>4</sub> in %	λ <sub>R</sub> (10 <sup>-3</sup> sec <sup>-1</sup> )	λ <sub>2</sub> (10 <sup>-5</sup> sec <sup>-1</sup> )	λ <sub>4</sub> (10 <sup>-5</sup> sec <sup>-1</sup> )	λ <sub>4</sub> /λ <sub>2</sub>
(-½, 2) → (½, 1)	S-1	-2.70	-0.20	1.7±0.5	10±3	43±7	4.3
	S-2	-2.39	-0.30	1.1±0.3	15±7	16±7	1.05
	S-3	-2.26	-0.22	1.9±0.5	16±3	33±3	2.04
(-½, -1) → (½, -2)	S-1	2.73	0.26	2.0±0.5	...	...	...
	S-2	2.92	0.27	1.0±0.5	7.0±0.5	31±5	4.44
	S-3	2.93	0.23	1.4±0.5	16±5	29±5	1.81
(-½, 0) → (½, -1)	S-1	2.55	-0.58	2.3±0.5	89.4	76.5	0.855
	S-2	2.22	-0.49	1.6±0.5	28±3	28±3	1.0
	S-3	2.19	-0.53	2.3±0.6	30±7	31±2	1.04
(-½, 1) → (½, -0)	S-1	-1.81	0.64	2.1±0.5	...	...	...
	S-2	-1.32	0.64	2.1±0.5	14±3	19±2	1.36
	S-3	-0.64	0.60	1.7±0.5	21±7	31±2	1.45

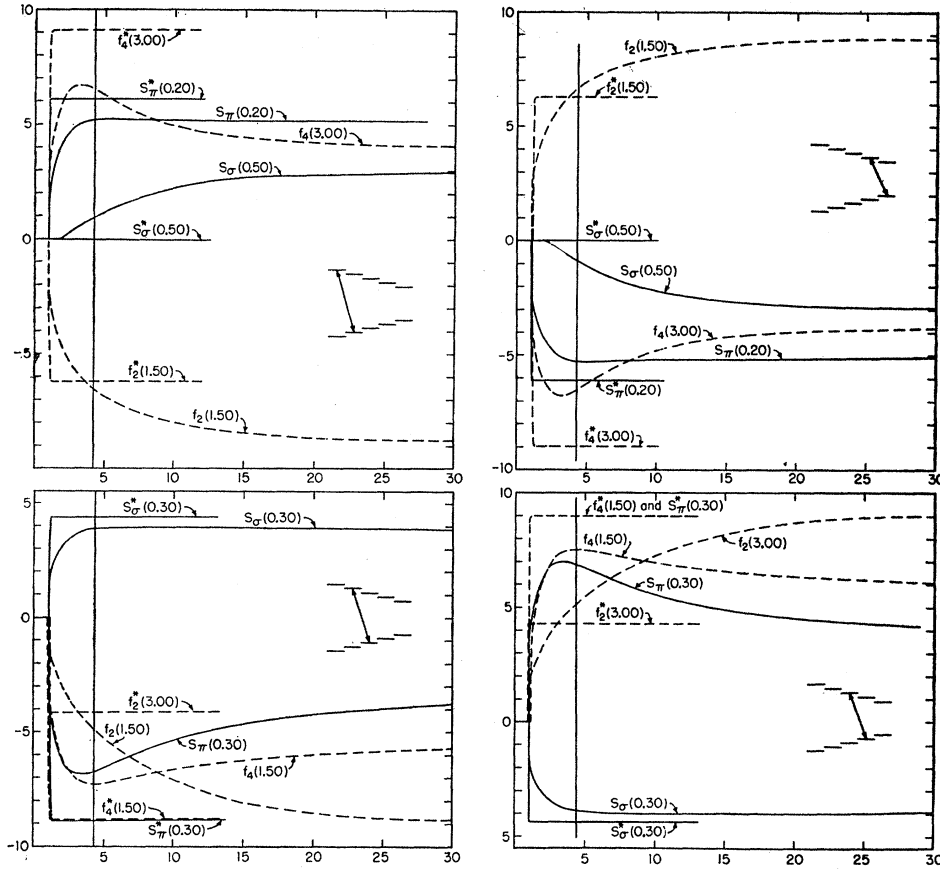


FIG. 8. A set of runs on the analog computer which shows the formation of the signals. For this run the circuit was as shown in Fig. 4, with  $R_1=100$  kohms,  $R_2=214$  kohms,  $c=20$  mf, and  $\alpha=0.4$ .  $S_\pi$  is the signal at  $0^\circ$  and  $S_\sigma$  the signal at  $90^\circ$ . The starred quantities are for the computer when  $R_1=0$ ,  $R_2=\infty$ . The figures in parentheses give the relative gain of the computer on the basis of full gain being 10. Full scale (+10) on the recorder corresponds to  $f_2=-2$ ,  $f_4=10$ ,  $S(0^\circ)=S_\pi=4$ , and  $S(90^\circ)=S_\sigma=-4$ . The vertical black line corresponds to the point in the experiment of which the saturating microwave field was turned off.

In order to calculate the  $B_2$  and  $B_4$ , the  $f_2$  and  $f_4$  must be known. The analog computer was used to determine  $f_2$  and  $f_4$  in terms of  $f_2^*$  and  $f_4^*$ , which are the  $f_2$  and  $f_4$  given by the simple no-nuclear-relaxation theory (Table I). The correction coefficients  $A_i$  are defined by

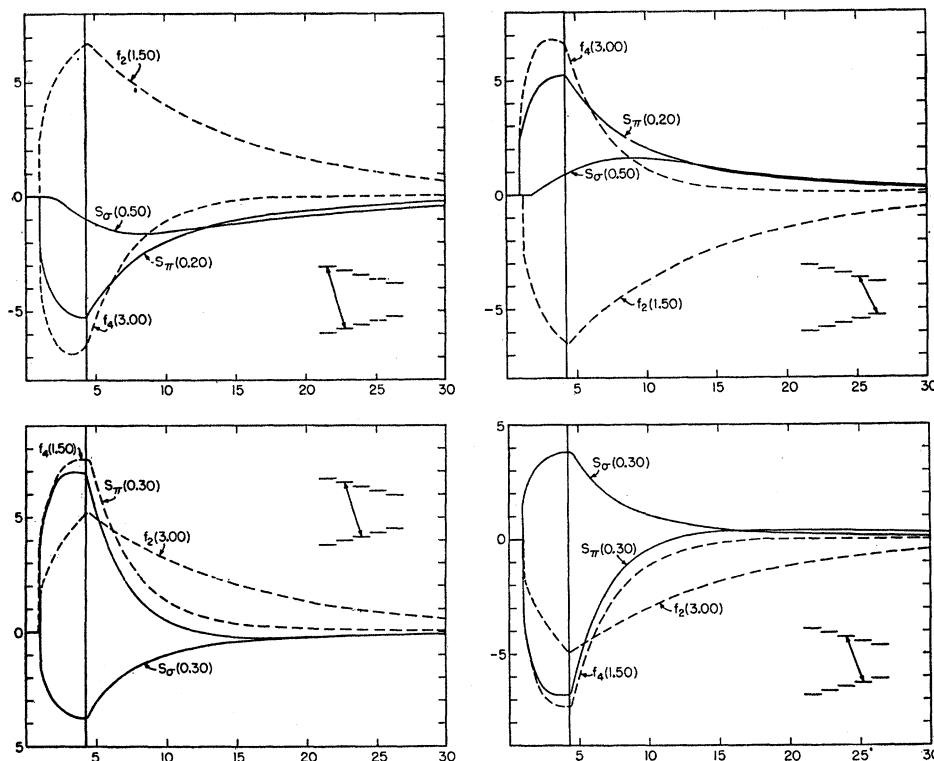
$$f_i = A_i f_i^*$$

The  $A_i$  were determined as follows: The quantities  $\lambda_2/\lambda_R$  and  $\lambda_4/\lambda_R$  were first calculated. Then it was assumed that the nuclear relaxation was due to a mixture of the modulation of the isotropic hyperfine interaction and the nuclear quadrupole interaction, and such a mixture was taken so as to reproduce the  $\lambda_2/\lambda_R$  and  $\lambda_4/\lambda_R$  values. The computer was then set

TABLE V. The time constants and their reproduced values. All time constants are expressed in terms of the rise time constant. The notation for the various transitions is as follows:  $\pi_{u_1}$ ,  $(-\frac{1}{2}, 2) \rightarrow (\frac{1}{2}, 1)$ ;  $\pi_l$ ,  $(-\frac{1}{2}, -1) \rightarrow (\frac{1}{2}, -2)$ ;  $\sigma_u$ ,  $(-\frac{1}{2}, 1) \rightarrow (\frac{1}{2}, 0)$ ;  $\sigma_l$ ,  $(-\frac{1}{2}, 0) \rightarrow (\frac{1}{2}, -1)$ . The column labeled "Run" refers to the transition from which the decay data were taken and the relaxation mechanism used to set up the computer. The  $W_2/W_3$  gives the relative contributions of dipole and quadrupole relaxation mechanisms.

Run	Quantity	Exp.	Simple theory	$\pi_u$	$\pi_l$	$\sigma_u$	$\sigma_l$	Average
S-1, $\pi_{u_1}$ , $W_3=0$	$\lambda_2$	5.9	6.24	5.47	5.44	4.81	5.74	5.37
	$\lambda_4$	25.1	20.8	19.7	18.0	18.9	20.1	19.2
	$\lambda_4/\lambda_2$	4.3	3.33	3.61	3.31	3.25	3.50	3.5
S-2, $\pi_{u_1}$ , $W_2/W_3=1.1$	$\lambda_2$	13.6	11.2	10.5	10.5	10.1	10.1	10.3
	$\lambda_4$	14.3	12.3	11.5	11.4	11.2	11.2	11.3
	$\lambda_4/\lambda_2$	1.05	1.10	1.10	1.09	1.11	1.11	1.10
S-2, $\pi_l$ , $W_3=0$	$\lambda_2$	7.0	7.87	6.78	7.27	6.54	7.03	6.90
	$\lambda_4$	31.0	26.2	22.9	21.8	22.8	25.2	2.32
	$\lambda_4/\lambda_2$	4.44	3.33	3.38	3.00	3.59	3.36	3.36
S-3, $\pi_l$ , $W_2/W_3=4.8$	$\lambda_2$	11.3	9.88	8.93	8.75	8.93	9.08	8.92
	$\lambda_4$	20.8	18.2	16.9	15.8	16.1	16.6	16.4
	$\lambda_4/\lambda_2$	1.81	1.84	1.89	1.81	1.80	1.83	1.84

FIG. 9. A set of runs on the computer which shows the formation and decay of the signals. The circuit values are the same as in Fig. 8.



up to duplicate this situation. The various transitions were run and the  $f_2$ ,  $f_4$ ,  $S(0^\circ)$  and  $S(90^\circ)$  recorded. The nuclear relaxation resistors were removed and the resistors representing the electron relaxation were shorted out. The signals observed with this arrangement gave a calibration with which to determine the  $A_i$  coefficients. To set up the computer only the relaxation data for the  $(-\frac{1}{2}, 2) \rightarrow (\frac{1}{2}, 1)$  and  $(-\frac{1}{2}, -1) \rightarrow (\frac{1}{2}, -2)$  transition were used. In case the measured relaxation times for these two transitions differed, a computer run was made for each of them. Figure 8 shows a typical run with the computer illustrating the formation of the signals. Figure 9 shows a run illustrating not only the formation but also the decay of the signals. The point at which the  $A_i$  were determined was selected by finding that time which corresponded to the point in the experiment at which the klystron was turned off. Table V gives a comparison between the time constants observed for the various transitions and those calculated on the basis of the simple theory which assumes predominance of the electron relaxation. Table VI gives the  $A_i$  coefficients which were determined for the various transitions.

Once the  $A_i$  have been determined, it is a simple matter to calculate the values of  $B_2$  and  $B_4$ . The results of these calculations are shown in Table VII. In order to check the consistency of the procedure, the calculated  $B_2$  and  $B_4$  were then used to set the computer so that it reproduced the observed signals.

Figure 10 shows a comparison between the observed signals and those reproduced in this fashion. A reproduction is shown for decay constants determined from both the  $(-\frac{1}{2}, 2) \rightarrow (\frac{1}{2}, 1)$  and  $(-\frac{1}{2}, -1) \rightarrow (\frac{1}{2}, -2)$  transitions; the  $B_2$  and  $B_4$  values were the averages of those obtained from these transitions.

INTERPRETATION OF THE RESULTS

It is clear from Table VI that essentially the same result is obtained for  $B_4$  from all the transitions and for all three sources; this is not true, however, of  $B_2$ . The value of  $B_2$  for the  $(-\frac{1}{2}, 0) \leftrightarrow (\frac{1}{2}, -1)$  transition is particularly erratic. The reason for this behavior is not known; a similar behavior was found for  $As^{76}$ . In particular, it is not clear whether this behavior indicates that all of the  $Sb^{122}$  atoms are not in the assumed donor sites or that there are some nuclear relaxation

TABLE VI.  $A_2$  and  $A_4$  correction factors. The notation for the various transitions is as follows:  $\pi_u$ ,  $(-\frac{1}{2}, 2) \rightarrow (\frac{1}{2}, 1)$ ;  $\pi_l$ ,  $(-\frac{1}{2}, -1) \rightarrow (\frac{1}{2}, -2)$ ;  $\sigma_u$ ,  $(-\frac{1}{2}, 1) \rightarrow (\frac{1}{2}, 0)$ ;  $\sigma_l$ ,  $(-\frac{1}{2}, 0) \rightarrow (\frac{1}{2}, -1)$ .

Relaxation data	$A_2$				$A_4$			
	$\pi_u$	$\pi_l$	$\sigma_u$	$\sigma_l$	$\pi_u$	$\pi_l$	$\sigma_u$	$\sigma_l$
S-1, $\pi_u$	1.15	1.16	1.36	1.33	0.78	0.77	0.85	0.88
S-2, $\pi_u$	0.95	0.97	0.94	0.96	0.96	0.94	0.93	0.93
S-2, $\pi_l$	1.08	1.08	1.20	1.23	0.75	0.73	0.83	0.82
S-3, $\pi_u$	1.03	1.09	1.20	1.28	0.91	0.83	0.88	0.92
S-3, $\pi_l$	1.00	1.01	1.04	1.05	0.84	0.84	0.87	0.88



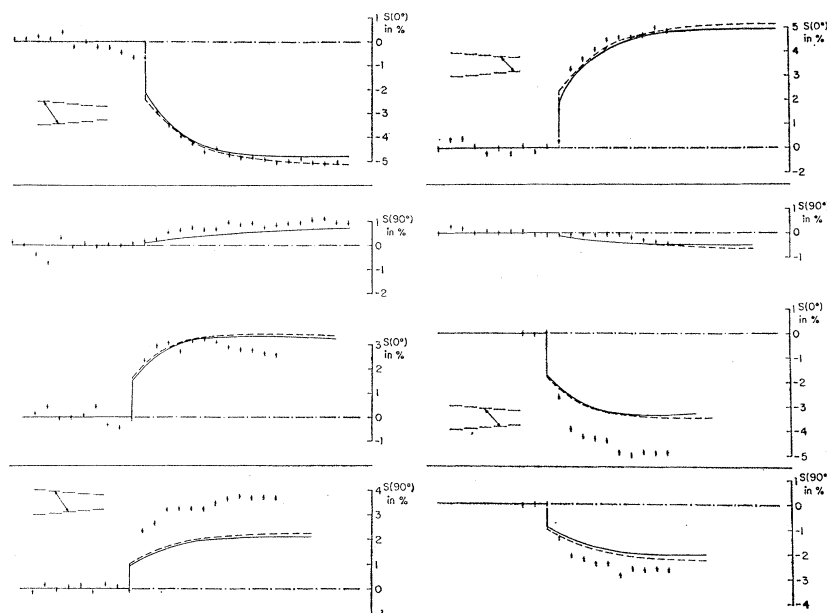


FIG. 10. A figure showing a comparison between the observed signals for S-3 and those which are reproduced by the computer. For the solid line the resistors were chosen to reproduce the average relaxation times observed for the  $(-\frac{1}{2}, 2) \rightarrow (\frac{1}{2}, -1)$  transition; for the dashed line, the  $(-\frac{1}{2}, -1) \rightarrow (\frac{1}{2}, -2)$  transition. The average values of the  $B_2$  and  $B_4$  obtained from both transitions were used.

processes in which the  $\text{Sb}^{122}$  donor interacts with other paramagnetic centers. For our analysis it will be assumed that only the  $B_2$  values from the outer  $[(-\frac{1}{2}, 2) \rightarrow (\frac{1}{2}, 1)$  and  $(-\frac{1}{2}, -1) \rightarrow (\frac{1}{2}, -2)]$  transitions are reliable. On this basis we conclude that

$$B_2/B_4 = 1.2 \pm 0.2,$$

$$B_4 = (0.37 \pm 0.05)/\eta.$$

The parameter  $\eta$  is an orientation efficiency; it is equal to the fraction of the  $\text{Sb}^{122}$  atoms which are in the simple donor sites depicted by the theory. From this experiment

$$0.32 \leq \eta \leq 1.$$

To see what this implies concerning  $\alpha_0$ ,  $\alpha_1$ , and  $\alpha_2$ , it is instructive to plot the line

$$\frac{B_2}{B_4} = \frac{1 - (\alpha_1/2) - (17\alpha_2/14)}{1 - (5\alpha_1/3) - (5\alpha_2/7)} = 1.2 \pm 0.2, \quad (20)$$

and the set of lines

$$B_4 = 1 - (5\alpha_1/3) - (5\alpha_2/7) = (0.37 \pm 0.05)/\eta$$

on the same graph. This plot is shown in Fig. 11. The shaded region gives those values of  $\alpha_0$ ,  $\alpha_1$ , and  $\alpha_2$  compatible with the results of this orientation experiment.

The data from the orientation experiment of Somoilov *et al.*<sup>13</sup> can be used to express  $B_2$  in terms of the unknown magnetic field  $H$  at the antimony nucleus in the iron sample. The result is

$$B_2 = \{[(1.9 \pm 0.2) \times 10^5 / H]\}^2.$$

If a value of  $H$  is assumed, then a value of  $B_2$  can be obtained. A set of lines for various values of  $H$  superimposed on the result for this experiment is shown in Fig. 12. From the two experiments we conclude that

$$170 \text{ kgauss} \leq H \leq 400 \text{ kgauss}.$$

If the nuclear resonance for a stable Sb nucleus in an iron sample could be found, light would be shed on both orientation experiments.

To secure further information concerning the nuclear matrix elements, it is necessary to take a closer look

TABLE VII. The  $B_2$  and  $B_4$  coefficients calculated for the various runs. The correction column shows the transition whose data were used to determine the nuclear relaxation times in order to correct for the effect of nuclear relaxation on the initial  $f_2$  and  $f_4$  parameters. The notation for the transitions is  $\pi_u, (-\frac{1}{2}, 2) \rightarrow (\frac{1}{2}, 1)$ ;  $\pi_l, (-\frac{1}{2}, -1) \rightarrow (\frac{1}{2}, -2)$ ;  $\sigma_u, (-\frac{1}{2}, 1) \rightarrow (\frac{1}{2}, 0)$ ;  $\sigma_l, (-\frac{1}{2}, 0) \rightarrow (\frac{1}{2}, -1)$ . The uncertainty in the determination of the  $B_2$  and  $B_4$  values is estimated to be 10 to 15%.

Source	Correction	$B_2$				$B_4$				$B_2/B_4$			
		$\pi_u$	$\pi_l$	$\sigma_u$	$\sigma_l$	$\pi_u$	$\pi_l$	$\sigma_u$	$\sigma_l$	$\pi_u$	$\pi_l$	$\sigma_u$	$\sigma_l$
S-1	$\pi_u$	0.43	0.43	0.74	1.07	0.34	0.44	0.49	0.43	1.26	0.98	1.51	2.49
S-2	$\pi_u$	0.38	0.44	0.64	1.03	0.33	0.30	0.37	0.28	1.15	1.47	1.73	3.68
S-2	$\pi_l$	0.34	0.41	0.50	0.82	0.43	0.38	0.43	0.32	0.79	1.08	1.16	2.56
S-3	$\pi_u$	0.32	0.40	0.24	0.76	0.26	0.30	0.35	0.30	1.23	1.33	0.69	2.53
S-3	$\pi_l$	0.34	0.44	0.29	0.95	0.29	0.30	0.36	0.32	1.17	1.47	0.81	2.97

at the beta-decay theory. In the notation of Kotani,<sup>18,19</sup> the six nuclear matrix elements which can contribute to a first-forbidden transition are

$$\eta w = C_A \int \boldsymbol{\sigma} \cdot \mathbf{r}; \quad \eta \xi' v = C_A \int i \gamma_5, \quad \lambda = 0$$

$$\eta u = C_A \int i \boldsymbol{\sigma} \times \mathbf{r}; \quad \eta \xi' y = -C_V \int i \boldsymbol{\alpha}; \quad \eta x = -C_V \int \mathbf{r}, \quad \lambda = 1$$

$$\eta z = C_A \int B_{ij}, \quad \lambda = 2.$$

The parameter  $\lambda$  gives the angular momentum carried off by the electron-neutrino system. Five of the matrix elements can be expressed in terms of the unique one  $z$  by choosing  $\eta$  so  $z=1$ . In the expressions for the spectrum shape, angular correlation, etc., there occur two particular combinations of matrix elements for which it

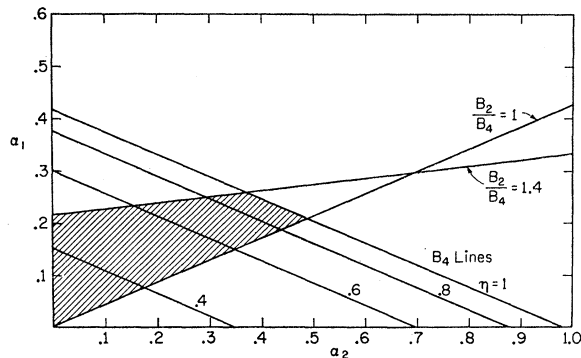


FIG. 11. A diagram showing the possible  $\alpha_1$  and  $\alpha_2$  which are compatible with this experiment. This restriction is based on the observed  $B_4$  and the  $B_2/B_4$  ratios for the two outer transitions.

is advantageous to introduce a special notation. These combinations are

$$V = \xi' v + \xi w, \quad \lambda = 0$$

$$Y = \xi' y - \xi(u+x), \quad \lambda = 1,$$

where  $\xi = \alpha Z / 2\rho$ ;  $\rho$  is the nuclear radius in units of the Compton wavelength,  $\alpha$  is the fine structure constant and  $Z$  the charge on the nucleus. For Sb<sup>122</sup>,  $\xi = 12.7$ . For our analysis the modified  $B_{ij}$  approximation will be used. This assumes that

$$z \neq 0, \quad Y \neq 0, \quad V \neq 0,$$

but

$$x = u = w = 0. \quad [Y, V < \xi].$$

In this approximation the shape factor for the beta spectrum is given by

$$C(W) = \{ Y^2 + V^2 + [(q^2 + \lambda_1 p^2) / 12] \},$$

<sup>18</sup> T. Kotani, Phys. Rev. **114**, 795 (1959).

<sup>19</sup> T. Kotani and M. Ross, Phys. Rev. **113**, 622 (1959).

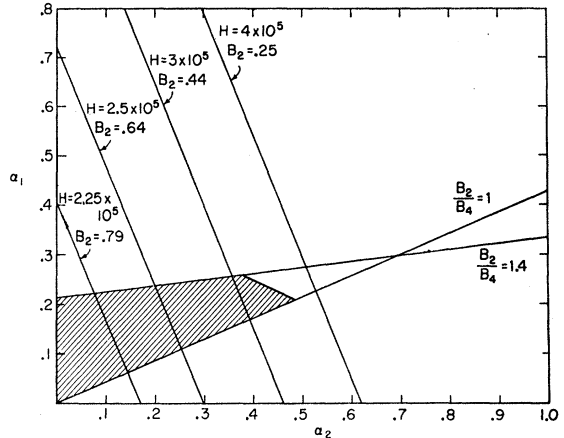


FIG. 12. A diagram showing the relationship between the orientation experiment of Somolov *et al.* and this one. From the two experiments we conclude that for Sb in iron 170 kgauss  $\leq H \leq 400$  kgauss.

where  $q$  is the neutrino momentum,  $p$  the electron momentum, and  $\lambda_1$  is a relativistic parameter which has been tabulated by Kotani and Ross.<sup>19</sup> In the  $B_{ij}$  approximation the values for  $\alpha_0$ ,  $\alpha_1$ , and  $\alpha_2$  are

$$\alpha_0 = V^2 / (V^2 + Y^2 + 0.521),$$

$$\alpha_1 = Y^2 / (V^2 + Y^2 + 0.521),$$

$$\alpha_2 = 0.521 / (V^2 + Y^2 + 0.521).$$

The normalization relationship between these parameters can be expressed in the form

$$V^2 + Y^2 = 0.521 [1/\alpha_2 - 1].$$

This equation together with Eq. (20) defines a locus in the  $V, Y$  plane of those points which are compatible with the observed orientation, that is, the shaded region in Fig. 11. Figure 13 shows this plot.

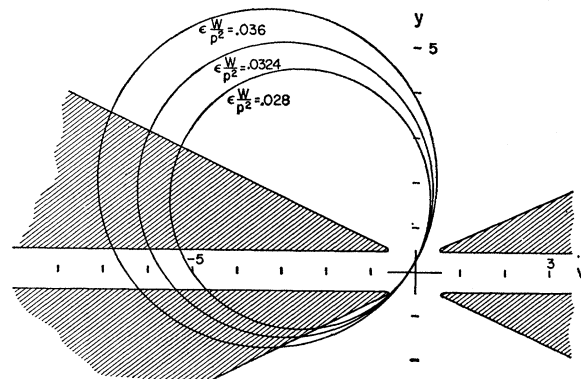


FIG. 13. A diagram showing the values of  $V$  and  $Y$  which are compatible with this orientation experiment and the observed angular correlation. For this analysis the modified  $B_{ij}$  approximation was used. *Note added in proof.* The labels for  $\epsilon(w/p^2)$  on the smallest and largest circles should be interchanged.

In terms of the  $B_{ij}$  approximation the  $\beta$ - $\gamma$  angular correlation is given by the expression<sup>18</sup>

$$1 + \epsilon P_2(\cos\theta),$$

where

$$\begin{aligned}\epsilon &= (p^2/W)(R_3k + eWk)/C(W), \\ R_3k &= \lambda_2(1/56)^{1/2}[Y - (8/3)^{1/2}V], \\ ek &= -(\lambda_1/112).\end{aligned}$$

The relationship between  $Y$  and  $V$  given by the angular correlation can be written in the form

$$\begin{aligned}\left[ V + \frac{\lambda_2}{2(21)^{1/2}\epsilon W/p^2} \right]^2 + \left[ Y - \frac{\lambda_2}{2(56)^{1/2}\epsilon W/p^2} \right]^2 \\ = \frac{11\lambda_2^2}{672[\epsilon W/p^2]^2} \frac{\lambda_1 W}{112\epsilon W/p^2} \frac{8^2 + \lambda_1 p^2}{12}.\end{aligned}$$

The three circles corresponding to the experimentally observed value and its limits of error are shown in Fig. 13. The overlap of these circles and the area given by the orientation experiment gives three regions of possible solution. These solutions are

$$V = -6.3 \pm 1.0,$$

$$Y = +1.8 \pm 1.5,$$

and

$$V = -4.2 \pm 2.0,$$

$$Y = -1.4 \pm 0.5,$$

and

$$V = -0.5 \pm 0.1,$$

$$Y = -0.5 \pm 0.1.$$

The first two of these imply that the orientation efficiency is  $\sim 40\%$ ; the third implies that the orientation is  $100\%$  efficient. The first two imply that for Sb in iron

$$H = 190 \text{ kgauss};$$

the third implies that for Sb in iron

$$H = 340 \text{ kgauss}.$$

#### DISCUSSION

At present there is insufficient evidence to decide between these three possibilities. We can only suggest additional experiments which would clarify the situation.

(1) Determination of the magnetic field at an antimony atom in an iron lattice. This could be done by a nuclear resonance method. Antimony is soluble in iron up to a concentration of a few percent. Experiments with  $\text{Fe}^{57}$  centers in such a lattice indicate that the nuclear resonance should be detectable. If this magnetic field could be found, then  $B_2$  could be found from the orientation experiment of Shakhov and consequently the orientation efficiency in our experiment.

(2) An improved measurement of the beta-gamma angular correlation as a function of energy. This would not only narrow the wide limits of the region of intersection, but it would also give a clue to the validity of the modified  $B_{ij}$  approximation.

(3) Measurement of the correlation between the direction of the beta ray and the circular polarization of the subsequent gamma ray. This gives an independent relationship between the nuclear matrix elements.

(4) A more precise measurement of the spectrum shape to see if the beta ray has a component with a unique forbidden shape.

#### ACKNOWLEDGMENTS

We are particularly indebted to Fong Chen for reducing the data, calculating the  $f_2$  and  $f_4$  parameters, and making the runs on the analog computer to correct for nuclear relaxation. We wish to thank Dr. Walter Brown and the Bell Telephone Laboratories for the gift of the doped silicon crystal.